

Optimization by Quantum Annealing: Lessons from Simple Cases

Lorenzo Stella,¹ Giuseppe E. Santoro,^{1,2} and Erio Tosatti^{1,2}

¹International School for Advanced Studies (SISSA),

and INFM Democritos National Simulation Center, Via Beirut 2-4, I-34014 Trieste, Italy

²International Centre for Theoretical Physics (ICTP), P.O. Box 586, I-34014 Trieste, Italy

(Dated: May 23, 2019)

This paper investigates the basic behavior and performance of simulated quantum annealing (QA) in comparison with classical annealing (CA). Three simple one dimensional case study systems are considered, namely a parabolic well, a double well, and a curved washboard. The time dependent Schrödinger evolution in either real or imaginary time describing QA is contrasted with the Fokker-Planck evolution of CA. The asymptotic decrease of excess energy with annealing time is studied in each case, and the reasons for differences are examined and discussed. The Husimi-Fisher classical power law of double well CA is replaced with a different power law in QA. The multi-well washboard problem studied in CA by Shinomoto and Kabashima and leading classically to a logarithmic annealing even in the absence of disorder, turns to a power law behavior when annealed with QA. The crucial role of disorder and localization is briefly discussed.

PACS numbers: 02.70.Ju, 02.70.Ss, 07.05.Tp, 75.10Nr

I. INTRODUCTION

The idea of quantum annealing (QA) is a late offspring of the celebrated simulated thermal annealing by Kirkpatrick et al¹. In simulated annealing, the problem of minimizing a certain cost (or energy) function in a large conformation space is tackled by the introduction of a fictitious temperature, which is slowly lowered in the course of a Monte Carlo or Molecular Dynamics simulation¹. This device allows an exploration of the conformation space of the problem at hand, effectively avoiding trapping at unfavorable local minima through thermal hopping above energy barriers. It makes for a very robust and effective minimization tool, often much more effective than standard, gradient-based, minimization methods.

An elegant and fascinating alternative to such a classical simulated annealing (CA) consists in helping the system escape the local minima through quantum mechanics, by tunneling through the barriers rather than thermally overcoming them^{2,3}. Experimental evidence in disordered Ising ferromagnets subject to transverse magnetic fields showed that this strategy is not only feasible but presumably winning in certain cases⁴. In essence, in quantum annealing one supplements the classical energy function, let us denote it by H_{cl} , with a suitable time-dependent quantum kinetic term, $H_{kin}(t)$, which is initially very large, for $t = 0$, then gradually reduced to zero in a time τ . The quantum state of the system $j(t)i$, initially prepared in the fully quantum ground state j_0i of $H(t=0) = H_{cl} + H_{kin}(0)$, evolves according to the Schrödinger equation

$$i\hbar\frac{d}{dt}j(t)i = [H_{cl} + H_{kin}(t)]j(t)i; \quad (1)$$

to reach a final state $j(t=\tau)i$. A crucial basic question is then how the residual energy $E_{res}(\tau) = E_{fin}(\tau) - E_{opt}$, decreases for increasing τ . Here E_{opt} is the absolute minimum of H_{cl} , and $E_{fin}(\tau)$ is the average energy attained by the system after evolving for a time τ , $E_{fin}(\tau) = \langle h(\tau) \rangle$. Generally speaking, this question has to do with the adiabaticity of the quantum evolution, i.e., whether the system is able, for sufficiently slow annealing (sufficiently long τ), to follow the instantaneous ground state of $H(t) = H_{cl} + H_{kin}(t)$, for a judiciously chosen $H_{kin}(t)$. The fictitious kinetic energy $H_{kin}(t)$ can be chosen quite freely, with the only requirement of being reasonably easy to implement. For this reason, this approach has also been called Quantum Adiabatic Evolution⁵.

At the level of practical implementations on an ordinary (classical) computer, the task of following the time-dependent Schrödinger evolution in Eq. 1 is clearly feasible only for toy models with a sufficiently manageable Hilbert space⁵. Actual optimization problems of practical interest usually involve astronomically large Hilbert spaces, a fact that calls for alternative stochastic (Quantum Monte Carlo) approaches. These QMC techniques, in turn, are usually suitable to using imaginary time quantum evolution, where the $i\hbar\theta_t$ in Eq. 1 is replaced by $\sim\theta$. One of the questions we will try to address in the present paper will be, therefore, if working with an imaginary-time Schrödinger evolution changes the quantum adiabatic evolution approach in any essential way. We will argue that, as far as annealing is concerned, imaginary-time is essentially equivalent to real time, and, as a matter of fact, can be quantitatively better.

Alternatively, a number of recent theoretical papers have applied Path-Integral Monte Carlo strategies to QA. A certain success has been obtained in several optimization problems, such as the folding of α -lattice polymer models^{6,7}, the random Ising model ground state problem^{8,9}, and the Traveling Salesman Problem¹⁰. It is fair to say, however, that there is no general theory predicting the performance of a QA algorithm, in particular correlating it with the energy landscape of the

given optimization problem. This is a quite unpleasant situation, in view of the fact that it is a-priori not obvious or guaranteed that a QA approach should do better than, for instance, CA. Indeed, for the interesting case of Boolean Satisfiability problems (more precisely, a prototypical NP-complete problem such as 3-SAT) recent attempts in our group showed that Path-Integral Monte Carlo annealing may perform slightly worse than simple CA¹¹.

Evidently, the performance of QA over CA depends in detail on the energy landscape of the problem at hand, in particular on the nature and type of barriers separating the different local minima, a problem about which very little is known in many practical interesting cases¹². It makes sense therefore to move one step back and concentrate attention on the simplest textbook problems where the energy landscape is well under control: essentially, one-dimensional potentials, starting from a double well potential, the simplest form of barrier. On these well controlled landscapes we can carry out a detailed and exhaustive comparison between quantum adiabatic Schrödinger evolution, both in real and in imaginary time, and its classical deterministic counterpart, i.e., Fokker-Planck evolution.

The rest of the paper is organized as follows. In Sec. II we define the problem we want to tackle, i.e., comparing Fokker-Planck annealing to Schrödinger annealing. In Sec. III we consider in detail the case of a double-well barrier. In Sec. IV we move to the case of a potential with many minima, but no disorder, where the behavior of classical and quantum annealing is remarkably different. In Sec. V the crucial role of disorder is discussed. Finally, Sec. VI contains a summary of the results found and a few concluding remarks. Details of the calculations are contained in the Appendices.

II. SCHRODINGER VERSUS FOKKER-PLANCK ANNEALING: STATEMENT OF THE PROBLEM

Suppose we are given a potential $V(x)$, (with x a Cartesian vector of arbitrary dimension), of which we need to determine the absolute minimum ($x_{\text{opt}}, E_{\text{opt}} = V(x_{\text{opt}})$). Assume generally a situation in which a steepest-descent approach, i.e., the strategy of following the gradient of V , would lead to trapping into one of the many local minima of V , and would thus not work. Classically, as an obvious generalization of a steepest-descent approach, one could imagine of performing a stochastic (Markov) dynamics in x -space according to a Langevin equation

$$\dot{x} = -\frac{1}{(T)} \nabla V(x) + \eta(t); \quad (2)$$

where the strength of the noise term is controlled by the squared correlations $\langle \eta_i(t) \eta_j(t') \rangle = 2D(T) \delta_{ij} \delta(t-t')$, with $D = 0$. Both $D(T)$ and $\langle \eta_i(t) \eta_j(t') \rangle$ (with dimensions of a diffusion constant and of a friction coefficient and related, re-

spectively, to fluctuations and dissipation in the system) are temperature dependent quantities which can be chosen, for the present optimization purpose, with a certain freedom. The only obvious constraint is in fact that the correct thermodynamical averages should be recovered from the Langevin dynamics only if $\langle T \rangle D(T) = k_B T$, an equality known as Einstein's relation¹³. Physically, $D(T)$ should be an increasing function of T , so as to lead to increasing random forces as T increases, with $D(T=0) = 0$, since noise is turned off at $T=0$. Classical annealing can in principle be performed through this Langevin dynamics, by slowly decreasing the temperature $T(t)$ as a function of time, from some initially large value T_0 down to zero. Instead of working with the Langevin equation (a stochastic differential equation) one might equivalently address the problem by studying the probability density $P(x;t)$ of finding a particle at position x at time t . The probability density is well known to obey a deterministic time-evolution equation given by the Fokker-Planck (FP) equation¹⁴:

$$\frac{\partial}{\partial t} P(x;t) = -\frac{1}{(T)} \nabla \cdot (\nabla P) + D(T) \nabla^2 P; \quad (3)$$

Here, the second term in the right-hand side represents the well-known diffusion term, proportional to the diffusion coefficient $D(T)$, whereas the first term represents the effect of the drift force ∇V , inversely proportional to the friction coefficient $\langle \eta_i(t) \eta_j(t) \rangle = k_B T \delta_{ij}$ ¹³. Annealing can now be performed, in principle, by keeping the system for a long enough equilibration time at a large temperature T_0 , and then gradually decreasing T to zero as a function of time, $T(t)$, in a given annealing time. We can model this by assuming

$$T(t) = T_0 f(t); \quad (4)$$

where $f(y)$ is some assigned monotonically decreasing function for $y \in [0;1]$, with $f(0) = 1$ and $f(1) = 0$. In this manner the diffusion constant D in Eq. (3) becomes a time-dependent quantity, $D_t = D(T(t))$. The FP equation should then be solved with an initial condition given by the equilibrium Boltzmann distribution at temperature $T(t=0) = T_0$, i.e., $P(x;t=0) = e^{-V(x)/k_B T_0}$. The final average potential energy after annealing in excess of the true minimum value, will then be simply given by:

$$E_{\text{res}} = \int dx V(x) P(x;t=0) = E_{\text{opt}}; \quad (5)$$

where E_{opt} is the actual absolute minimum of the potential V .

In a completely analogous manner, we can conceive using Schrödinger's equation to perform a deterministic quantum annealing (QA) evolution of the system, by studying:

$$\frac{\partial}{\partial t} \langle x \rangle(t) = -\langle t \rangle \nabla^2 V(x) + \langle x \rangle(t); \quad (6)$$

where $\langle \cdot \rangle = i$ for a real time (RT) evolution, while $\langle \cdot \rangle = 1$ for an imaginary time (IT) evolution. Here $\langle t \rangle =$

$\omega^2 = 2m_t$ will be our annealing parameter, playing the role that the temperature $T(t)$ had in classical annealing. Once again we may take $T(t)$ varying from some large value ω_0 at $t=0$ (corresponding to a small mass of the particle, hence to large quantum fluctuations) down to $T(t=\infty) = 0$, corresponding to a particle of infinite mass, hence without quantum fluctuations. Again, we can model this with $T(t) = \omega_0 f(t/\omega_0)$, where f is a preassigned monotonically decreasing function. A convenient initial condition here will be $P(x; t=0) = \omega_0(x)$, where $\omega_0(x)$ is the ground state of the system at $t=0$, corresponding to the large value $T(t=0) = \omega_0$ and hence to large quantum fluctuations. For such a large ground state will be isolated, and separated by a large energy gap from all excited states. The residual energy after annealing will be similarly given by Eq. (5), where now, however, the probability $P(x; t=\infty)$ should be interpreted as

$$P(x; t) = \frac{\int_{-\infty}^{\infty} j(x; t) dx}{\int_{-\infty}^{\infty} j(x_0; t) dx} :$$

In general, the residual energy will be different for a RT or an IT Schrödinger evolution. We will discuss in some detail RT versus IT Schrödinger evolution in Sec. III A.

The basic question we pose is which annealing scheme is eventually more effective, leading to the smallest final residual energies $\text{res}(\infty)$. This might seem an ill-posed question, because the time scales involved in the classical and in the quantum evolution are different, and also because, practically, the two approaches might involve different computational costs which would imply different CPU time scales. In other words, it might seem that it only makes sense to ask how well an annealing scheme performs in a given CPU time T_{CPU} , with all the unavoidable uncertainty associated to a CPU time-related answer (involving, among other things, the programmer's skills, the algorithmic choices, and the computer architecture). We will show, however, that the behavior of $\text{res}(\infty)$ can be so vastly different for the different schemes, obviously in strict relation with the form of the potential, that such time scale concerns are often practically irrelevant¹⁵.

A. The harmonic potential: a warm-up exercise

Preliminary to any further treatment of a potential with barriers, and as a warm-up exercise which will be useful later on, we start here with the simple case of a parabolic potential in one dimension, $V(x) = kx^2/2$, which has a trivial minimum in $x=0$, with $E_{\text{opt}}=0$, and no barriers whatsoever.

Let us consider classical FP annealing first. As detailed in the Appendix, it is a matter of simple algebra to show that, for the harmonic potential, one can write a simple closed linear differential equation¹⁶ for the average

potential energy $\text{pot}(t)$, which has the form :

$$\frac{d}{dt} \text{pot}(t) = k D_t^{-1} \frac{2}{k_B T(t)} \text{pot}(t) ; \quad (7)$$

the initial condition being simply given by the equipartition value $\text{pot}(t=0) = k_B T_0/2$. As with every one-dimensional linear differential equation, Eq. (7) can be solved by quadrature for any choice of $T(t)$ and $D_t = D(T(t))$. Assuming the annealing schedule to be parameterized by an exponent $\tau > 0$, $T(t) = T_0(1-t/\omega_0)^\tau$, being the annealing time, and the diffusion constant $D(T)$ to behave as a power law of temperature, $D(T) = D_0(T=T_0)^\alpha$ with $\alpha > 0$, we can easily extract from the analytical solution for $\text{pot}(t)$ the large asymptotic behavior of the final residual energy $\text{res}(\infty) = \text{pot}(t=\infty)$. That turns out to be:

$$\text{res}(\infty) \stackrel{\text{CA}}{\sim} \frac{T}{T(D-1)+1} : \quad (8)$$

Trivial as it is, annealing proceeds here extremely fast, with a power-law exponent CA that can increase without bounds (for instance if $\alpha = 1$) upon increasing the exponent τ of the annealing schedule.

Consider now the Schrödinger evolution problem for this potential,

$$\frac{\partial}{\partial t} \langle x; t \rangle = -i(t) r^2 + \frac{k}{2} x^2 \langle x; t \rangle \quad (9)$$

$$\langle x; t=0 \rangle = \omega_0(x) ;$$

where $\omega_0(x) / \exp(-B_0 x^2/2)$ is the ground state Gaussian wavefunction corresponding to the initial value of the Laplacian coefficient $\langle t=0 \rangle = \omega_0$, and $i = i_r$ or $= i_i$ for a real time (RT) or an imaginary time (IT) evolution, respectively. This problem is studied in detail in the Appendix, where we show that a Gaussian Ansatz for $\langle x; t \rangle$, of the form $\langle x; t \rangle / \exp(-B_t x^2/2)$ with $\text{Re}(B_t) > 0$, satisfies the time-dependent Schrödinger equation as long as the inverse variance B_t of the Gaussian satisfies the following ordinary non-linear first-order differential equation:

$$B_t = k \frac{2}{r} \frac{\langle t \rangle B_t^2}{\frac{k}{2} \langle B_t \rangle} \quad (10)$$

$$B_{t=0} = B_0 = \frac{k}{2 \omega_0} :$$

Contrary to the classical case, there is no simple way of recasting the annealing problem in terms of a closed linear differential equation for the average potential energy $\text{pot}(t)$. The final residual energy $\text{res}(\infty) = \text{pot}(t=\infty)$ is still expressed in terms of B (or better, of its real part $\langle B \rangle$),

$$\text{res}(\infty) = \frac{\int_{-\infty}^{\infty} V(x) j(x; t=\infty) dx}{\int_{-\infty}^{\infty} j(x; t=\infty) dx} = \frac{k}{4 \langle B \rangle} ; \quad (11)$$

but the behavior of B must be extracted from the study of the non-linear equation (10). The properties of the solutions of Eq. (10) are studied in detail in the Appendix, where we show that:

i) $\text{res}(\cdot)$ cannot decrease faster than $1 =$, for large \cdot , i.e., a power-law exponent $\text{res}(\cdot)$ is bound to be $\text{QA} = 1$.

ii) Adopting a power-law annealing schedule $(t) = 0(1 - t =)$, the exponent QA for the IT case is

$$\text{QA} = \frac{1}{1 + 2}; \quad (12)$$

increasing towards the upper bound 1 as \cdot is increased towards 1.

iii) RT quantum annealing proceeds with exactly the same exponent QA as IT quantum annealing (although $\text{res}^{\text{RT}}(\cdot) = \text{res}^{\text{IT}}(\cdot)$ in general), except that the limit $\lim_{\cdot \rightarrow 1} \text{res}(\cdot) = 1$ (abrupt switch-off of the Laplacian coefficient) is singular in the RT case.

Summarizing, we have learned that, for a single parabolic valley in configuration space, both CA and QA proceed with power-laws, but CA can be much more efficient than QA, with an arbitrarily larger power-law exponent. We underline however that this is merely an academic matter at this point, steepest descent being much more efficient than both CA and QA in such a simple case. The power of QA shows up only when potentials with barriers are considered.

III. THE SIMPLEST BARRIER: A DOUBLE-WELL POTENTIAL

Let us take now the classical potential to be optimized as a simple double-well potential in one-dimension

$$V_{\text{sym}}(x) = V_0 \frac{(x^2 - a^2)^2}{a^4} + x; \quad (13)$$

with V_0 , a , and \cdot real constants. In absence of the linear term ($\cdot = 0$), the potential has two degenerate minima located at $\pm a$, and separated by a barrier of height V_0 . When a small linear term $\cdot > 0$ is introduced, with $a \ll V_0$, the two degenerate minima are split by a quantity $\cdot = 2a$, the minimum at $x = -a$ becoming slightly favored. For reasons that will be clear in a moment, it is useful to slightly generalize the previous potential to a less symmetric situation, where the two wells possess definitely distinct curvatures at their minimum (i.e., their widths differ substantially). This is realized easily, with a potential of the form:

$$V_{\text{asym}}(x) = \begin{cases} V_0 \frac{(x^2 - a_+^2)^2}{a_+^4} + x & \text{for } x \geq 0 \\ V_0 \frac{(x^2 - a_-^2)^2}{a_-^4} + x & \text{for } x < 0 \end{cases}; \quad (14)$$

with $a_+ \neq a_-$, both positive. (The discontinuity in the second derivative at the origin is of no consequence in our discussion.) To linear order in the small parameter \cdot , the two minima are now located at $x = \pm a \approx \pm \sqrt{8V_0}$,

the splitting between the two minima is given by $\cdot = (a_+ + a_-)$, while the second derivative of the potential at the two minima, to lowest order in \cdot , is given by:

$$V''(x = \pm a) = \frac{8V_0}{a^2};$$

Obviously, V_{sym} is recovered if we set $a_+ = a_- = a$ in V_{asym} .

We now present the results obtained by the annealing schemes introduced in Sec. II above. The Fokker-Planck and the Schrödinger equation (both in RT and in IT) were integrated numerically using a fourth-order Runge-Kutta method, after discretizing the x variable in a sufficiently fine real space grid¹⁷. For the FP classical annealing, the results shown are obtained with a linear temperature schedule, $T(t) = T_0(1 - t =)$ (i.e., $\cdot = 1$), and a diffusion coefficient simply proportional to $T(t)$, $D_t = D_0(1 - t =)$ (i.e., $\text{D} = 1$). Consequently, the friction coefficient is kept constant in t , $\cdot = k_B T(t) = D_t = k_B T_0 = D_0$. Similarly, for the Schrödinger quantum annealing we show results obtained with a coefficient of the Laplacian (t) vanishing linearly in time, $\text{Q}(t) = 0(1 - t =)$ (i.e., $\text{Q} = 1$).

Fig. 1 shows the results obtained for the quenched probability distribution $P(x; t =)$ at different values of \cdot , for both the Fokker-Planck (CA, panel (a)) and the Schrödinger imaginary-time case (IT, panel (b)), for a symmetric double well potential $V_{\text{sym}}(x)$, with $V_0 = 1$ (our unit of energy), $a = a_+ = a_- = 1$ (unit of length), $\text{D} = 0.1$. Fig. 1(c) summarizes the results obtained for the residual energy $\text{res}(\cdot)$. Fig. 2(a,b,c) shows the corresponding results for an asymmetric double well potential, Eq. 14, with $a_+ = 1.25$, $a_- = 0.75$, and $\cdot = 0.1$.

We notice immediately that QA wins, in both cases, over CA for large enough value of \cdot . The RT-QA behaves as its IT counterpart for the symmetric double well, while it shows a different behavior in the asymmetric case (see below for comments). To go deeper into the details of the different evolutions, let us begin discussing the CA data (panel (a) and (c) of Figs. 1 and 2), which show similar behaviors for both choices of the potential. Starting from an initially broad Boltzmann distribution at a high $T = T_0 = V_0$, $P(x; t = 0)$ (solid lines), the system quickly sharpens the distribution $P(x; t)$ into two well-defined and quite narrow peaks located around the two minima x of the potential. This agrees very well with expectations based on the CA in a harmonic potential, which showed that the width of the Gaussian should decrease linearly in Q ($\text{CA} = 1$ for $\text{D} = 1$), as is indeed found in our double well case too. If we denote by p the integral of each of the two narrow peaks, with $p_+ + p_- = 1$, it is clear that the problem has effectively been reduced to a discrete two-level system problem. The time evolution p therefore obeys a discrete Master equation which involves the thermal promotion of particles over the barrier V_0 , of the form:

$$\frac{1}{\text{dt}} \frac{dp_+}{dt} = [1 - p_-(t)] e^{-\frac{V_0 + B}{k_B T(t)}} p_-(t) e^{-\frac{B}{k_B T(t)}}; \quad (15)$$

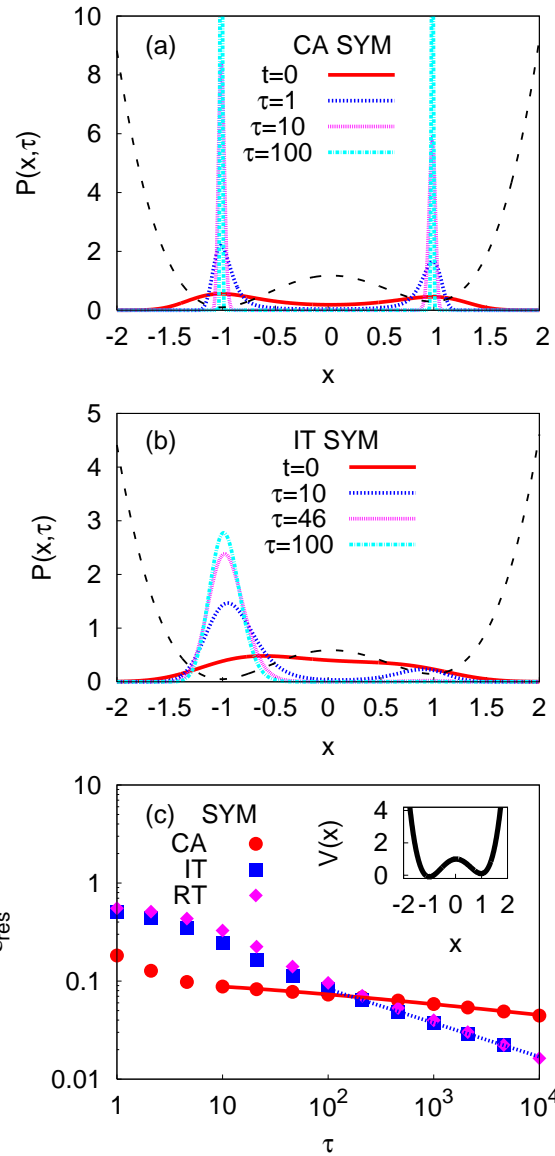


FIG. 1: (a,b): The annealed probability distribution $P(x; t = \tau)$ at different values of the annealing time τ , for both the Fokker-Planck classical annealing (CA, panel (a)), and the Imaginary Temperature Schrödinger quantum annealing (IT-QA, panel (b)). (c) Final residual energy $\epsilon_{\text{res}}(\tau)$ versus annealing time τ for quantum annealing in Real Temperature (RT) and Imaginary Temperature (IT) compared to the Fokker-Planck classical annealing (CA). The solid line in (c) is a fit of the CA data. The double well potential (dashed line in (a,b), inset of (c)) is here given by Eq. (14) with $a_+ = a_- = a = 1$.

where ω is an attempt frequency, while $B = V_0 - V(x_0)$ and $B + v = V_0 - V(x_+)$ are the potential barriers seen from a particle in the metastable minimum, x_0 , and in the true minimum, x_+ , respectively. Eq. (15) was studied by Huse and Fisher in Ref. 18, where they showed that the asymptotic value of the residual energy $\epsilon_{\text{res}}(\tau) =$

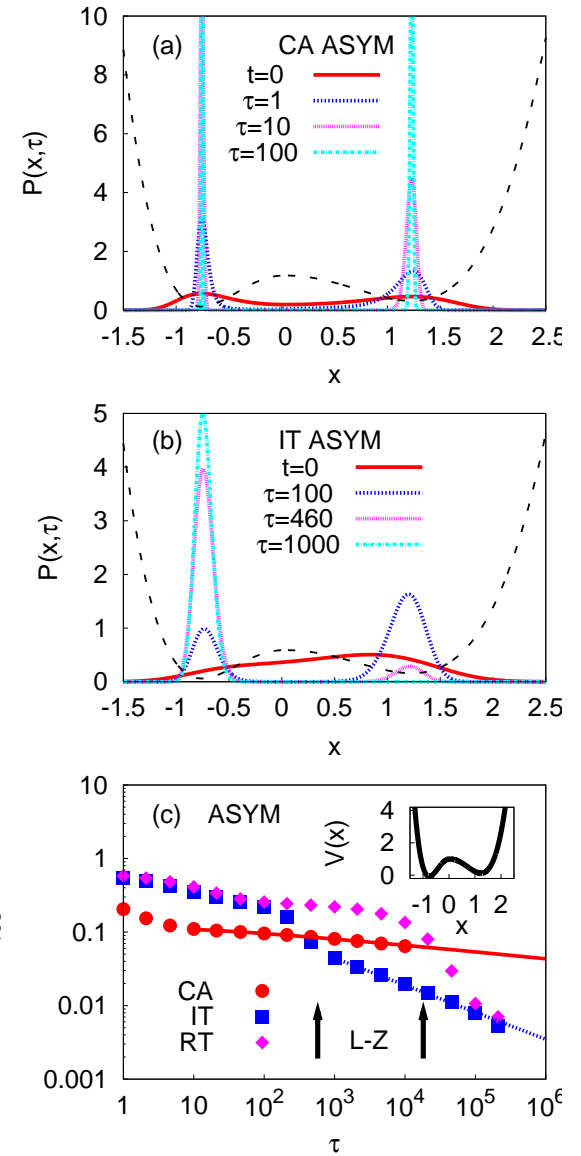


FIG. 2: Same as Fig. 1, for the asymmetric potential in Eq. (14) with $a_+ = 1.25; a_- = 0.75$ (dashed line in (a,b), inset of (c)). Notice the different behavior of RT and IT, in the present case.

$p_+(\tau)$ is given by:

$$\epsilon_{\text{res}}(\tau) \sim \text{const}(\tau)^{\frac{v}{B}} (\ln \tau)^{\frac{2-v}{B}}; \quad (16)$$

where \sim is a constant. So, apart from logarithmic corrections, the leading power-law behavior is of the form $\epsilon_{\text{res}} \sim \tau^{\frac{v}{B}}$, where the exponent is controlled by the ratio v/B between the energy splitting of the two minima v and the barrier B . As shown in Figs. 1(c) and 2(c) (solid lines through solid circles), the asymptotic behavior anticipated by Eq. (16) fits nicely our CA residual energy data (solid circles), as long as the logarithmic corrections are accounted for in the fitting procedure¹⁹.

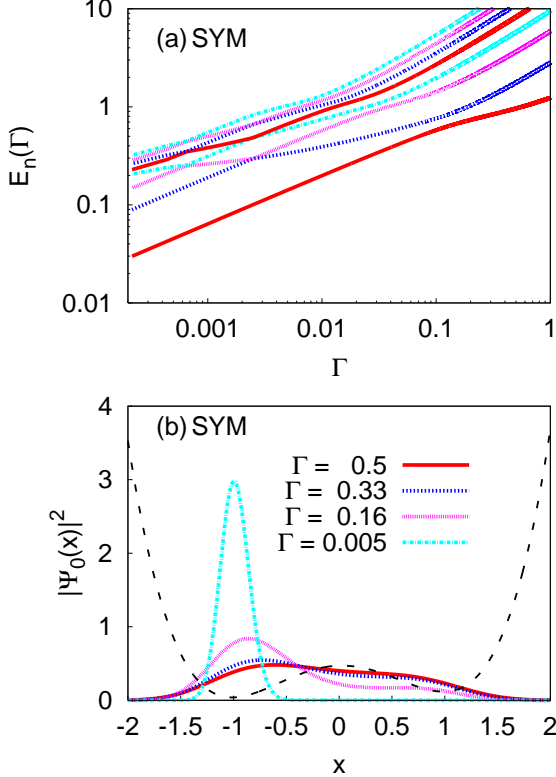


FIG. 3: Instantaneous eigenvalues (a) and ground state wavefunctions (b) of the Schrödinger problem $H = E$ for different values of Γ , for the symmetric potential in Eq. (14) with $a_+ = a_- = a = 1$.

Obviously, we can make the exponent as small as we wish by reducing the linear term coefficient α , and hence the ratio $v = B$, leading to an exceedingly slow classical annealing.

The behavior of the QA evolution is remarkably different. Starting from Fig. 1, we notice that IT and RT evolutions give very similar residual energies, definitely faster decaying than the CA data, while the corresponding final wavefunction only slowly narrows around the minimum of the potential. Notice also the asymptotic behavior of the residual energy, $E_{\text{res}}(\Gamma) \sim \Gamma^{1/3}$, indicated by the dashed line in Fig. 1(c): this rather strange exponent is simply the appropriate one for the Schrödinger annealing with a linear schedule within an harmonic potential (the lower minimum valley, see Sec. II A). The asymmetric potential results, shown in Fig. 2, are even more instructive. The initial wavefunction squared $|\Psi_0(x; t=0)|^2$ corresponds to a quite small mass (a large $\alpha = 0.5$), and is broad and delocalized over both minima (solid line). As we start annealing, and if the annealing time is relatively short (that is, if $\Gamma < \Gamma_c$, with a characteristic time Γ_c which depends on which kind of annealing, RT or IT, we perform), the final wavefunction becomes mostly concentrated on the wrong minimum, roughly corresponding to the ground state with a still relatively large

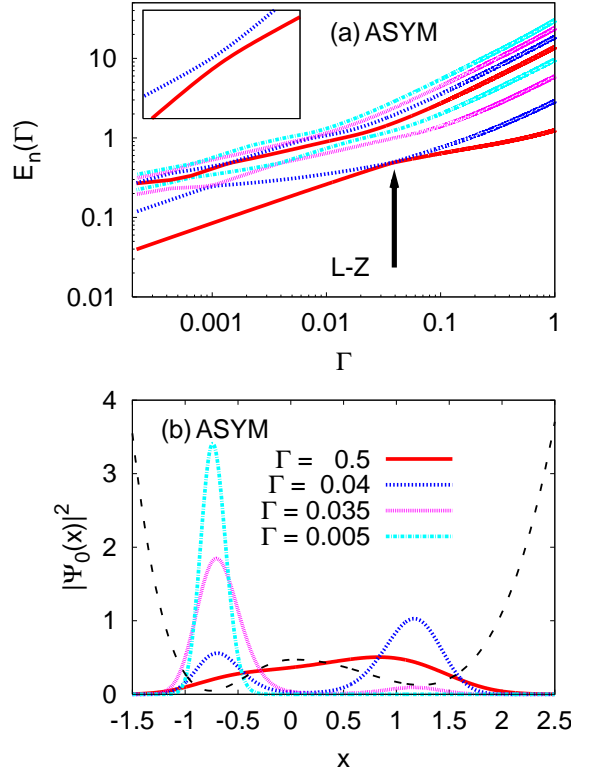


FIG. 4: Same as Fig. 3, for the asymmetric potential in Eq. (14) with $a_+ = 1.25$; $a_- = 0.75$. Notice the clear Landau-Zener avoided crossing in (a), indicated by the arrow and magnified in the inset.

$\Gamma_c < \Gamma_0$ (see Fig. 4). The larger width of the wrong valley is crucial, giving a smaller quantum kinetic energy contribution, so that tunneling to the other (deeper) minimum does not yet occur. By increasing Γ , there is a crossover: the system finally recognizes the presence of the other minimum, and effectively tunnels into it, with a residual energy that, once again, decays asymptotically as $E_{\text{res}}(\Gamma) \sim \Gamma^{1/3}$ (dashed line in Fig. 2(c)). There is a characteristic annealing time Γ_c different in the two Schrödinger cases, RT and IT, above which tunneling occurs, and this shows up as the clear crossover in the residual energy behavior of both IT and RT, shown in Fig. 2(c).

These findings can be quite easily rationalized by looking at the instantaneous (adiabatic) eigenvalues and eigenstates of the associated time-independent Schrödinger problem, which we show in Fig. 4(a,b). Looking at the instantaneous eigenvalues shown in Fig. 4(a) we note a clear avoided-crossing occurring at $\Gamma = \Gamma_{\text{LZ}} = 0.038$, corresponding to a resonance condition between the states in the two different valleys of the potential. For $\Gamma > \Gamma_{\text{LZ}}$ the ground state wavefunction is predominantly concentrated in the wider but metastable valley, while for $\Gamma < \Gamma_{\text{LZ}}$ it is mostly concentrated on the deeper and narrower global minimum valley. In the full

time-dependent RT evolution, transfer to the lower valley is a Landau-Zener problem^{20,21}: the characteristic time τ_c for the tunneling event is given by $\tau_{LZ} = \sim \frac{1}{\alpha_0^2} \frac{2}{\Delta^2}$, where α is the relative slope of the two crossing branches as a function of x , Δ is the gap at the avoided-crossing point, and α_0 is the initial value of the annealing parameter. (For the case shown in Fig. 4, we have $\alpha = 0.0062$, $\Delta = 2.3$, hence $\tau_{LZ} = 18980$, see rightmost arrow in Fig. 2(c).) The Landau-Zener probability of jumping, during the evolution, from the ground state onto the "wrong" (excited) state upon fast approaching of the avoided level crossing is $P_{ex} = e^{-\tau_{LZ}}$, so that adiabaticity applies only if the annealing is slow enough, $\tau_c > \tau_{LZ}$.

The IT characteristic time τ_c is smaller, in the present case, than the RT one. We will comment further on this point in Sec. IIIA. In a nutshell, the reason for this is the following. After the system has jumped into the excited state, which occurs with a probability $P_{ex} = e^{-\tau_{LZ}}$, the residual IT evolution will filter out the excited state; this relaxation towards the ground state is controlled by the annealing rate as well as by the average gap seen during the residual evolution. Numerically, the characteristic time τ_c seen during the IT evolution is of the order of $\sim (2)$, see leftmost arrow in Fig. 2(c), rather than being proportional to $1 = \Delta^2$ as τ_{LZ} would imply.

Obviously, instantaneous eigenvalues/eigenvectors can be studied for the Fokker-Planck equation as well; their properties, however, are remarkably different from the Landau-Zener scenario just described for the Schrödinger case. Fig. 5(c) shows the first four low-lying eigenvalues of the FP equation as a function of T (for a symmetric choice of the potential), while Fig. 5(a,b) show the corresponding eigenstates for two values of the temperature, $T=V_0 = 1$ and $T=V_0 = 0.1$. (The asymmetric potential cases are virtually identical, and are not shown). The lowest eigenvalue of the FP operator is identically 0 and the corresponding eigenvector¹⁴ is the Boltzmann distribution $e^{-V(x)/k_B T}$, with roughly symmetric maxima on the two valleys. The first excited state correspond to distribution peaked on the two valley but with a node at the origin, and is separated from the ground state by an exponential small Arrhenius-like gap $e^{-B/k_B T}$. Higher excited states are separated by a very large gap, so that, effectively, only the two lowest lying states dominate the dynamics at small temperature. The reduction of a continuum double-well FP classical dynamics onto a discrete effectively quantum two-level system, previously noticed, is quite evident from this form of the spectrum. On the contrary, the true quantum case never allowed for a discrete two-level system description whatsoever, except perhaps for large Δ . For small enough $\Delta < \tau_{LZ}$, in particular, the tower of oscillator states within the valley at $x = 0$ is always very close in energy to the actual ground state, and the quantum annealing evolution reduces effectively to a particle in a single harmonic well. This explains the rather large width of the final distributions $P(x)$ observed in the quantum case.

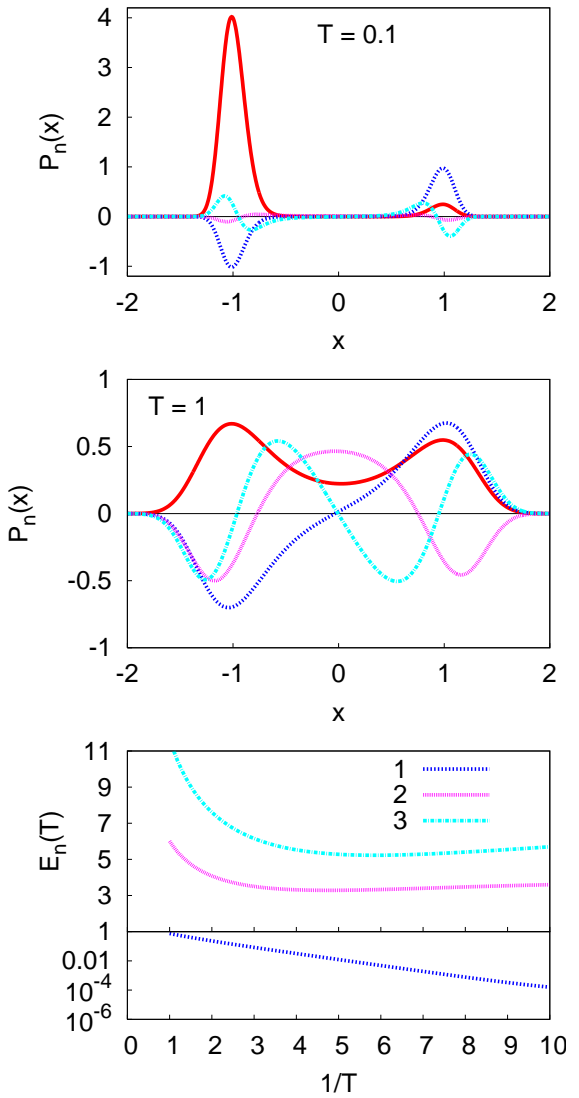


FIG. 5: Instantaneous Fokker-Planck eigenvalues (panel (c)) as a function of temperature T , and the corresponding eigenstates for two values of T (panels (a) and (b)). The potential is here the symmetric one, V_{sym} in Eq. 13 with $V_0 = 1$, $a = 1$, $\Delta = 0.1$. Similar results (not shown) are obtained for the asymmetric double-well potential V_{asym} .

Summarizing, we have found that QA and CA proceed in a remarkably different way. CA is sensitive to the height of the barrier, more precisely to the ratio $v = B$ between the energy offset v of the two minima, and the barrier height B . On the contrary, QA crucially depends on the tunneling probability between the two valleys, which is reflected in a Landau-Zener (avoided crossing) gap: a wide tunneling barrier is obviously bad for QA. Finally, we noticed that RT and IT proceed with somewhat different characteristic times: we discuss this issue a bit more in the following section.

A . Real-versus imaginary-time Schrodinger evolution

A Schrodinger dynamics in imaginary-time (IT) is clearly much more convenient than that in real-time (RT) for simulations on current classical computers, but it makes a difference in the final results? The answer to this question is, we believe: no, it does not make a difference, in essence, although IT does give quantitatively better results.

To qualify this statement, let us denote by $j^{(\cdot)}(t)i$ the solution of the Schrodinger equation

$$\frac{d}{dt}j^{(\cdot)}(t)i = [H_{cl} + H_{kin}(t)]j^{(\cdot)}(t)i$$

$$j^{(\cdot)}(t_0)i = j_0i \quad (17)$$

where we assume that j_0i is the ground state of the initial Hamiltonian at time t_0 , $H_{cl} + H_{kin}(t_0)$, while $\gamma = \hbar$ for RT or $\gamma = 1$ for IT. By definition, the final residual energy after annealing up to time $t_f = t_0 + \tau$, where the kinetic energy is finally turned on, is given by:

$$E_{res}^{(\cdot)} = \frac{h^{(\cdot)}(t_0 + \tau)H_{cl}j^{(\cdot)}(t_0 + \tau)i}{h^{(\cdot)}(t_0 + \tau)j^{(\cdot)}(t_0 + \tau)i} \quad E_{opt} : \quad (18)$$

We conjecture that the residual energies for the two alternative way of doing a Schrodinger evolution verify the following: i) the IT residual energy is not larger than the RT one, that is

$$E_{res}^{(IT)} \leq E_{res}^{(RT)}; \quad (19)$$

and ii) in many problems, the leading asymptotic behavior, for $\tau \gg 1$, might be identical for $E_{res}^{(IT)}$ and $E_{res}^{(RT)}$.

Expectation (i) seems very reasonable: it is simply inspired by the time-independent case, where it is well known that the IT Schrodinger dynamics tends to "lter the ground state" out of the initial trial wave function, as long as the gap between the GS and the first excited state is non-zero. However, we have here a time-dependent situation, and the result is a priori not guaranteed. We do not have a proof of this statement, but we have verified it in all the cases where an explicit integration of the Schrodinger equation has been possible (see, for instance, the results of the previous Section). (Needless to say, we have no proof of (ii) either, but, again, it never failed in all our tests.)

The simplest time-dependent problem where one can test our conjectures, is the discrete two-level system (TLS) problem. Here, in terms of Pauli matrices, $H_{cl} = z$, while $H_{kin}(t) = x(t)$, with $x(t) = vt$. The full $H(t)$ is therefore

$$H(t) = z - x(t)x : \quad (20)$$

The annealing interpretation is very simple: the classical optimal state is $j\#i$, with energy $E_{opt} = z$, separated

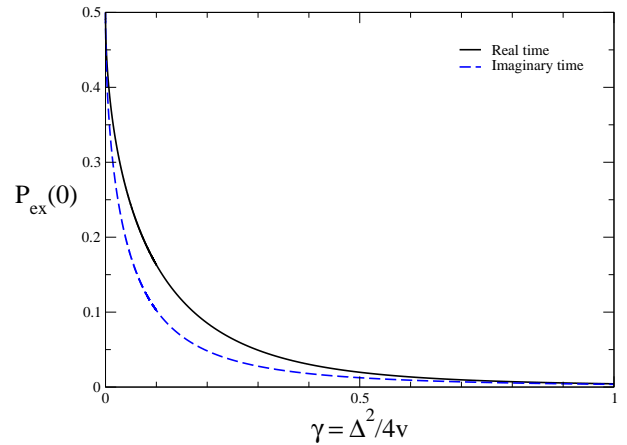


FIG. 6: The probability $P_{ex}(0)$ of ending up into the excited state, given by Eq. 21, for the discrete two-level system problem in Eq. 20, for both imaginary-time (IT, dashed line) and real-time (RT, solid line) Schrodinger annealing. The large- behavior of $P_{ex}(0)$ is, in both cases, given by $P_{ex}(0) \sim 1/(256\gamma^2)$.

from the excited state $j''i$ by a gap $2z$. The kinetic term induces transitions between the two classical states. Starting from the ground state of $H(t_0)$ at time $t_0 = 0$, we let the system evolve up to time $t_f = t_0 + \tau = 0$, when the Hamiltonian is entirely classical, $H(t_f = 0) = H_{cl} = z$. The probability of missing the instantaneous ground state $j\#i$, ending up with the excited state $j''i$, is: $P_{ex}(0) = |j''i|^2 = |h^{(\cdot)}(0)j^{(\cdot)}(0)i|^2$. In principle, P_{ex} depends, for given γ , both on the initial state $j(t_0) = j_0 = v$ and on the annealing time τ . The really important parameter, however, turns out to be the ratio v between these two quantities, which determines the "velocity of annealing": Taking $\tau \gg 1$ (i.e., $t_f \gg 1$), and $j_0 = 1$ with $j(t) = vt$ for every t , the problem can be solved analytically (in terms of parabolic cylinder functions, see for instance Ref. 3 for the RT case) for both RT and IT. The probability $P_{ex}(0)$ of ending into the excited state can be expressed in terms of the variable $R = \gamma^2 = 4v$. The explicit expressions, in terms of Gamma functions, are:

$$P_{ex}(0) = \frac{\Re + 1/\Re}{2(1 + \Re^2)} \quad (21)$$

$$R = e^{i\pi/4} \frac{1}{P} = \frac{(1+z)}{(1+2z)};$$

where $j_0 = 3 = 4$ and $z = i$ for RT, while $j_0 = 1$ and $z = 0$ for IT. A plot of P_{ex} for both RT and IT is shown in Fig. 6 as a function of $\gamma = \Delta^2 / 4v$. Note that: i) the IT result for P_{ex} (dashed line) is always below the RT result, ii) the difference between the two curves is only quantitative: one can verify analytically that the leading behavior for large γ is the same in both cases, i.e., $P_{ex} \sim 1/(256\gamma^2)$. Similar results are obtained by direct numerical integration of the Schrodinger equation for finite τ and v , and with other forms of $x(t)$.

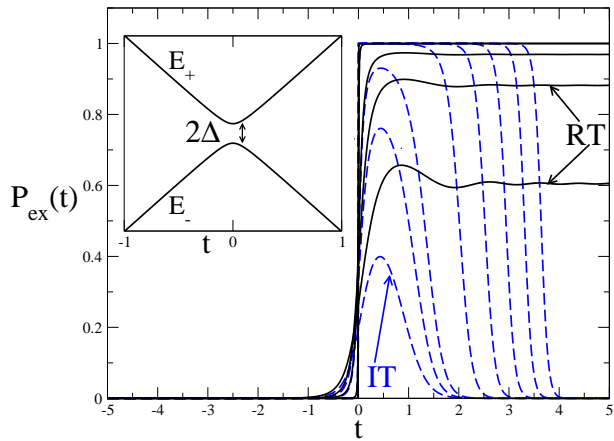


FIG. 7: Comparison between the RT (solid lines) and the IT (dashed lines) evolution of a Landau-Zener problem, Eq. 22, for several values of the tunneling gap 2 (the values of 2 shown are $= 0.4; 0.2; 0.1; 10^{-2}; 10^{-3}; 10^{-4}; 10^{-5}; 10^{-6}$, while $v = 1$). The inset shows the two instantaneous eigenvalues of the problem, $E_{\pm}(t)$, as a function of t .

With the same toy model, we can illustrate another point raised in the previous Section: what happens to the IT evolution after a Landau-Zener avoided crossing gap is encountered. The Hamiltonian we consider is essentially that in Eq. 20, simply rotated in spin space,

$$H(t) = vt^z \quad x : \quad (22)$$

In absence of the tunneling amplitude, the two energy levels would cross at $t = 0$, while for $z > 0$ the two instantaneous eigenvalues are simply $E_{\pm}(t) = \pm \sqrt{(vt)^2 + 2}$ (see inset in Fig. 7). Starting with the system in the ground state at $t = -1$, we can monitor the probability of getting onto the excited states at any time t , which we plot in Fig. 7 for both the RT and the IT evolution and for several values of 2 (taking $v = 1$). The RT data provide an illustration of the well-known Landau-Zener result: after a (relatively short) tunneling time, and possibly a few oscillations, the probability of getting onto the excited state saturates to a value given by $P_{ex}(t = 1) = e^{-2/\sim v}$. As for the IT data, the initial (tunneling) part and the subsequent plateau of the curves are similar to the RT case: the plateau value attained, call it P_{ex} , is indeed very close to the RT saturation value (in fact, asymptotically the same for $2 \neq 0$); after that, the IT evolution starts to filter out the ground state component $\{$ initially present in the state with a small amplitude $1 - P_{ex}$ $\}$ through the usual mechanism of suppression of excited states, leading to a $P_{ex}(t)$ which is nicely fit by the curve

$$P_{ex}(t) = \frac{P_{ex} e^{-2 \int_0^t dt^0 [E_+(t^0) - E_-(t^0)]}}{(1 - P_{ex}) + P_{ex} e^{-2 \int_0^t dt^0 [E_+(t^0) - E_-(t^0)]}} ; \quad (23)$$

which asymptotically goes to zero as $t \rightarrow 1$. This rather

trivial effect of filtering, if on one hand explains the discrepancy between the IT and the RT evolution observed

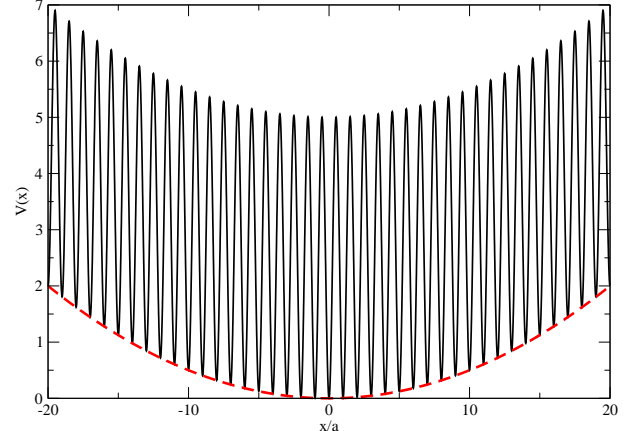


FIG. 8: Parabolic washboard potential resulting in a logarithmically slow classical annealing. The minima are regularly located at positions $x_i = ia$, and the dashed line shows the parabolic envelope potential.

in the asymmetric double well case of the previous section, is, on the other hand, of no harm at all: on the contrary, it provides a quantitative improvement of IT over RT.

In summary, the essential equivalence of IT and RT Schrödinger annealing (with, moreover, a quantitative improvement of IT over RT) justifies practical implementations of quantum annealing based on imaginary-time Quantum Monte Carlo schemes.

IV. ONE-DIMENSIONAL CURVED WASHBOARD: A POTENTIAL WITH MANY MINIMA

After discussing at length the annealing problem in a potential with one minimum and with two minima, we wish to move on to a multi-minima problem, however simple. There are simple but interesting one-dimensional potentials which allow us to do that. The first example was proposed and solved by Shinomoto and Kabashima in Ref. 16, and consists in a parabolically shaped washboard potential. This example will display a logarithmically slow classical annealing, showing CA may run into trouble even in simple models with no complexity whatsoever, whereas quantum mechanics can do much better in this case. Consider a wiggly one-dimensional potential with barriers of individual height B separating different local minima, regularly located a distance a apart one from each other, i.e., at positions $x_i = ai$. The i th-local minimum is at energy $E_i = ka^2 i^2/2$, so that the resulting envelope is parabolic. In order to study the dynamics of a particle in this potential, a good starting point is to write the master equation for the probability $P_i(t)$ that the particle is in the i th-valley at time t :

$$-\frac{1}{dt}P_i(t) = P_{i+1}(t)e^{-B_{i+1;i}} + P_{i-1}(t)e^{-B_{i-1;i}} - P_i(t)e^{-B_{i;i+1}} - e^{-B_{i;i-1}}; \quad (24)$$

where τ is an attempt frequency, $B_{i;j}$ is the effective barrier from i to j , and $\tau = 1/k_B T$. This is a well justified starting point, in view of the results of the previous sections (Sects. III and IIIA), showing that classical annealing is extremely fast in reducing the width of a probability distribution within each valley to an essentially delta-function like sequence of peaks of strength P_i . The actual form of the effective barriers depends on the way we model the details of the potential, with the only constraint that detailed balance is satisfied, i.e.,

$$B_{i;i+1} = B_{i+1;i} = \dots = B_i = \dots = B_{i-1};$$

in such a way that the stationary solution, for constant T , is simply the Boltzmann probability distribution, $P_i(t) = 1 / \exp(-E_i/k_B T)$. Ref. 16 takes $B_{i+1;i} = B_{i-1;i} = B$, while $B_{i;i+1} = B + \tau_i$ and $B_{i-1;i} = B + \tau_{i-1}$, with $\tau_i = \tau_{i+1} = \tau$. The potential energy of the valleys enters only through the $B_{i;j}$, which control the probability of making transitions between valleys.

In order to study Eq. (24), Shinomoto and Kabashima introduced a continuum limit, by defining a macroscopic coordinate x , such that the minima are at $x_i = ia$, and writing the equation governing the probability $P(x; t)$ in the limit $\tau \ll 0$. The derivation involves writing $P_{i-1}(t)$ in terms of derivatives of $P(x; t)$, keeping consistently terms up to order a^2 and expanding exponentials with the assumption that $k_B T = (ka^2) \gg 1$. The continuum limit equation governing the evolution of $P(x; t)$ turns out to be a Fokker-Planck (FP) equation, Eq. (3), with an effective diffusion constant of the form

$$D_e(T) = a^2 e^{-B/k_B T}; \quad (25)$$

$D_e(T) = k_B T = D_e(T)$, and an effective drift potential $V(x) = kx^2/2$ given by the macroscopic parabolic envelope potential. In order to study the annealing properties of the system, one can then follow exactly the same steps leading to Eq. (7), which applies here too, except that now D_e is substituted by $D_e(T)$, which has an exponential activated behavior, $D_e(T) \propto e^{-B/k_B T}$. This exponentially activated $D_e(T)$ changes the annealing behavior in a drastic way. Recall that the CA exponent α_{CA} of Sect. (IIA) decreases towards zero as the exponent D in the relationship $D(T) \propto T^D$ increases. Since, close to $T = 0$, $e^{-B/k_B T} \ll T^D$ for any arbitrarily large D , we could suspect that the behavior of $\tau_{res}(t)$ will no longer be a power law. In fact, the surprising result of this exercise¹⁶ is that the optimal annealing schedule $T(t)$ is logarithmic and that $\tau_{res}(t)$ converges to 0 at best as²²

$$\tau_{res}(t) \propto \log(t)^{-1}; \quad (26)$$

The reason behind this result is that the time derivative of $\tau_{res}(t)$ becomes exponentially small as one anneals T towards 0, due to the presence of $e^{-B/k_B T}$ in the diffusion constant, and an exponentially small derivative brings (not surprisingly) a logarithmically slow decrease of the function. To put it more physically, consider solving Eq. (7) for a time independent T ; the solution is trivially

$$\tau_{res}(t) = C e^{-t/t_{relax}} + \frac{k_B T}{2} \quad t_{relax} = \frac{k_B T}{2 ka^2} e^{B/k_B T};$$

We observe that the solution converges to the equilibrium (equipartition) value $k_B T = 2$ exponentially with a characteristic time t_{relax} which itself increases exponentially fast with decreasing T . As a result, the system will never be able to follow the decreasing T till the end of the annealing, by maintaining roughly the equilibrium value $\tau_{pot} = k_B T = 2$. Indeed, if we assume for instance $T(t) = T_0(1 - t)$, the relaxation of the system will cease to be effective (i.e., the system will fall out of equilibrium) at a time t , and temperature $T = T(t)$, at which $t_{relax} = \tau$, i.e., when $k_B T = B = \log 2$. The residual energy at this point cannot be smaller than the equipartition value $k_B T = 2$, hence $\tau_{res} = B = \log 2$ as well. This freezing and falling out of equilibrium for classical system with barriers seems to provide an ubiquitous source of logarithms in classical annealing¹⁸.

How would one tackle this annealing problem quantum mechanically? As the quantum analog of the master equation Eq. (24), we propose studying the Schrödinger evolution governed by a tight-binding Hamiltonian with on-site energies E_i and hopping matrix-elements between adjacent sites $h_{i;i+1}$

$$H = \sum_i \frac{c_i^\dagger c_i}{2} + \sum_i h_{i;i+1} c_i^\dagger c_{i+1} + c_{i+1}^\dagger c_i : \quad (27)$$

The justification and possible limitations of this starting point, over the actual original continuum problem will be discussed at the end of the section. Here it is enough to consider that the hopping matrix-elements $h_{i;i+1}$ depend on tunneling through the barrier separating i from $i+1$. The precise form of $h_{i;i+1}$ is likely to be inessential, including its energy (and hence site) dependence, for which we will assume the semi-classical (WKB) form:

$$h_{i;i+1} = h_0 \frac{V_h}{a} e^{-\frac{1}{4} \frac{P}{V_h}}; \quad (28)$$

$= \sim^2 = (2m a^2)$ being simply related to the quantum confinement energy of a particle of mass m in a valley of size a . Here h_0 and V_h are energy parameters related to the details of the potential and of the barrier, which

will play little or no role. If the mass of the particle m (and hence $h_{i,i+1}$) is kept constant the particle will explore the potential due to the kinetic term in the Hamiltonian: the correspondence between the quantum and the classical formulation is that ϵ plays the role of T , $h_{i,i+1}$ plays the role of the classical transition probabilities, the ground state wavefunction $j_i^{(GS)}$ at a given value of ϵ (or, equivalently, of the hopping term h) plays the role of the classical equilibrium Boltzmann distribution $P_i^{(T\text{eq})}$. The question, once again, is how to anneal, by reducing it as a function of time $\epsilon_i(t)$, in such a way as to squeeze the wavefunction of the system so that the average potential energy

$$P_{\text{pot}}(t) = \frac{\sum_i \epsilon_i(t) j_i^2}{\sum_i j_i^2} \quad (29)$$

is minimal.

As it turns out, the continuum limit is once again useful. One goes to the continuum exactly as in the FP case by using $x_i = a_i$, writing $\langle x_i; t \rangle = \epsilon_i(t) = a_i$ and expanding everything to order a^2 . When written in first quantized form, the Hamiltonian for the quantum particle in the macroscopic continuum coordinate x is simply

$$H(t) = \epsilon(t) r^2 + V(x) \quad (30)$$

where the coefficient of the Laplacian ϵ is the quantum counterpart of the classical effective diffusion constant D_ϵ

$$\epsilon(t) = a^2 h(t) = a^2 h_0 \frac{V_h}{(t)}^{1/4} e^{-\frac{P}{V_h}(t)}; \quad (31)$$

and $V(x) = kx^2/2$, as in the classical case. The continuum limit quantum problem has therefore exactly the form we have considered in Sec. (IIA), except that $\epsilon(t)$ in Eq. (10) is now substituted by an effective Laplacian coefficient ϵ which has a highly non-linear, in fact exponential, dependence on the annealing parameter (t) . We know, however, from Sec. (IIA), that a non-linear behavior of the type $(1-t)$ for the Laplacian coefficient leads to a power-law decrease of $\epsilon_{\text{res}}(t)$ with an exponent η_A which is, remarkably, an increasing function of ϵ , approaching 1 as $\epsilon \rightarrow 1$. Therefore, contrary to the classical case, where an exponentially activated behavior of the diffusion constant D_ϵ is strongly detrimental to the annealing (turning a power law into a logarithm), here the exponential WKB-like behavior of ϵ will do no harm at all. Indeed, we numerically integrated the relevant equation for B_t , Eq. (10) with ϵ in place of ϵ , using the exponential WKB expression Eq. (31) for ϵ while annealing $\epsilon(t)$ with a linear schedule, $\epsilon(t) = \epsilon_0(1-t)$. The integration was performed, as usual, with a fourth-order Runge-Kutta method, and was carried on up to time $t=1$, when the kinetic term in the Hamiltonian ceases to exist. The numerical results (not shown) have a clear power-law behavior for the quantum annealed (QA) final residual

energy $\epsilon_{\text{res}}(t=1)$, with a power law exponent η_A which is compatible with 1. Once again, the exponent appears to be insensitive to the choice of the type of quantum evolution (RT versus IT), although the numerical values of residual energies always respect the inequality $\epsilon_{\text{res}}^{\text{RT}}(1) \leq \epsilon_{\text{res}}^{\text{IT}}(1)$.

Before ending this section, we would like to discuss briefly the reason for treating by tight-binding, Eq. 27, what was originally a continuum problem with a well defined potential landscape. As we learned from the double-well case, there is never a clear-cut discrete model (a discrete two-level system, in that case) describing in a complete way the continuum Schrödinger problem, in all stages of the annealing. Obviously, when the mass of the particle is very small, the tight-binding approximation contained in Eq. 27 is not particularly good, since more than one state per valley is generally important to describe the wavefunction accurately. As the mass of the particle increases, however, the tight-binding approach gets more and more appropriate, until a further limitation appears: when the mass is very large, it is not legitimate to neglect excited states within, say, the central valley compared to the lowest states localized in metastable valleys. We can imagine that the ultimate behavior of $\epsilon_{\text{res}}(t)$, in the quantum case, will be actually dominated by the rather trivial problem of squeezing the wavefunction in the lowest central minimum, with its characteristic power-law exponent ($1/3$, for instance, for a linear schedule). There is, however, an intermediate region, between the very short scale, where the full details of the potential are important, and the very long scale, where the trivial squeezing mentioned above sets in, and where the tight-binding approximation reasonably predicts a power-law exponent (of order 1) for $\epsilon_{\text{res}}(t)$.

We believe that one of the important points that makes QA so different from CA in the present case is that the spectrum of the instantaneous eigenvalues of the quantum problem does not show any dangerous Landau-Zener avoided-crossing, and, correspondingly, the ground state wavefunction is always more peaked in the central valley than elsewhere. As in the two-level case, a disorder in the width of the different valleys would change this result.

V. ROLE OF DISORDER

Despite their disarming simplicity, the three case studies above turn out to be extremely informative in qualifying the profound difference of QA from CA, and their surprising consequences. We expect that these results will be very important in understanding more realistic QA problems. Of course, the cases studied, although instructive, do not possess the real ingredient which makes annealing difficult, both in CA and QA, i.e., some form of disorder in the distribution of the minima. We believe, for instance, that even an irregular landscape with many minima, as the double-cosine potential $V(x) =$

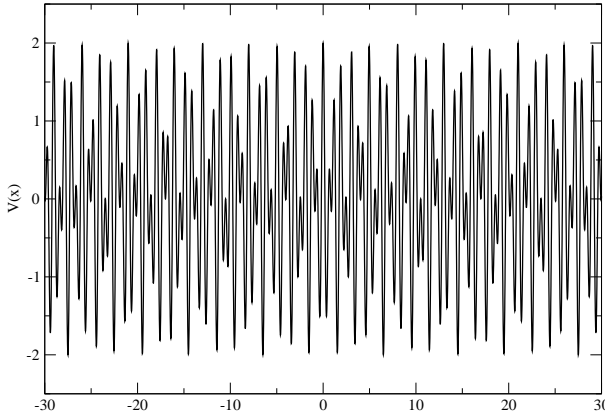


FIG. 9: Double cosine potential $V(x) = \cos(2x) + \cos((1+5)x)$, showing an irregular landscape with many minima.

$V_1 \cos(2x) + V_2 \cos(2rx)$ (with r an irrational number) shown in Fig. V, would already change drastically the behavior of QA from a power-law to a logarithm. On quite general grounds, Anderson's localization²³ would predict that wavefunctions are localized for a genuinely disordered potential for large enough mass (i.e., small enough kinetic energy bandwidth) in any $D > 2$ (this localization occurs for all value of the mass in $D = 1; 2$). Therefore, quantum annealing should always, via a cascade of Landau-Zener events, end up into some localized state which has, a priori, nothing to do with our search of the actual potential minimum.

A very simple illustration of the crucial role of disorder is given by the $D = 1$ disordered Ising ferromagnet:

$$H = \sum_i J_i \frac{z_i z_j}{z_i + z_j} \quad (32)$$

where $J_i > 0$ are positive random variables in the interval $[0; 1]$, and z is the transverse field inducing quantum fluctuations. Obviously, the ground state is the ferromagnetic state with all spins aligned up (or down). However, arbitrarily weak values of the J_i can pin domain walls between up and down ferromagnetic regions, with a very small energy cost $2J_i$. For a finite system with periodic boundary conditions domain walls appear in pairs, and separate sections of the system with alternating "up" and "down" ferromagnetic ground states. Given two domain walls pinned at weak- J_i points a distance $L \gg 1$ apart, healing the system via single spin flip moves requires flipping L spins, which can be a formidable barrier to tunnel through. The system will have a very slow annealing (quantum, as well as classical) while showing, at the same time, no complexity whatsoever: simple disorder is enough.

VI. SUMMARY AND CONCLUSIONS

Summarizing, we have compared Schrödinger versus Fokker-Planck annealing in various simple cases of one-

dimensional potential, in particular a double well potential and a parabolic washboard potential with many minima but no disorder. In all cases the two annealings, quantum and classical, were seen to behave in a remarkably different way. Classical annealing is influenced only by the height of the barriers surrounding the relevant minima, via Arrhenius-like thermal promotion over the barriers, with probability distributions which are quite localized on those minima. Quantum annealing is influenced by the structure of the eigenvalue spectrum of the problem (very small Landau-Zener tunneling gaps associated to large barriers are highly detrimental to it). In some cases, for instance in the case of the parabolic washboard potential, quantum annealing can be much more effective than classical annealing, but, generally speaking, both strategies suffer whenever the potential landscape is disordered. As an outcome of the discussion, it is quite clear that quantum annealing, although potentially useful and sometimes more convenient than classical annealing, is not capable, in general, of finding solutions of NP-complete problems in polynomial time: indeed, quite interestingly, even trivial optimization problems (trivial, obviously, only from the complexity point of view), like the one-dimensional ferromagnetic random Ising model, can

Acknowledgments

This project was sponsored by MIUR through FIRB RBAU017S8R004, FIRB RBAU01LX5H, COFIN 2003 and COFIN 2004, and by INFM ("Iniziativa trasversale calcolo parallelo"). We acknowledge illuminating discussions with Domenico Battaglia.

APPENDIX A: ANNALING IN A PARABOLIC POTENTIAL

1. Classical Annealing (Fokker-Planck) case.

It is straightforward to find the solution of the Fokker-Planck Eq. (3) when the potential is harmonic, $V(x) = kx^2/2$, and the initial condition is the Boltzmann distribution $P(x; t=0) \propto \exp(-kx^2/(2k_B T_0))$. Indeed, it is simple to verify that the Gaussian Ansatz

$$P(x; t) = C_t e^{-B_t x^2}; \quad (A1)$$

fulfills the initial condition (if $B_{t=0} = B_0 = k/(2k_B T_0)$) and solves the FP equation, as long as the two functions B_t and C_t satisfy the following ordinary differential equations:

$$\begin{aligned} & \frac{d}{dt} B_t = 2D_t \frac{k_B T}{k_B T(t)} - \frac{2B_t^2}{k_B T(t)} \quad : \\ & \frac{d}{dt} C_t = D_t \frac{k}{k_B T(t)} - \frac{2B_t}{k_B T(t)} \quad : \end{aligned} \quad (A2)$$

The normalization constant C_t turns out to be irrelevant in calculating the average potential energy which we need

$$p_{\text{pot}}(t) = \frac{\int_{\mathbb{R}} \frac{dxV(x)P(x;t)}{dxP(x;t)}}{\int_{\mathbb{R}} dxP(x;t)} = \frac{k}{4B_t}; \quad (\text{A } 3)$$

and can be completely forgotten, since the equation for B_t does not involve it. The equation for B_t appears to be non-linear, but can immediately be transformed into a linear equation by dividing up both sides by B_t^2 and recognizing that the correct variable to use is precisely $1=B_t$, or better yet, $p_{\text{pot}}(t)$. In terms of $p_{\text{pot}}(t)$ we can therefore write a linear equation of the form :

$$\frac{d}{dt} p_{\text{pot}}(t) = kD_t - 1 - \frac{2}{k_B T(t)} p_{\text{pot}}(t); \quad (\text{A } 4)$$

the initial condition being simply given by the equipartition value $p_{\text{pot}}(t=0) = (k=4B_0) = k_B T_0/2$. An alternative way¹⁶ of deriving Eq. (A 4) consists in taking the derivative with respect to time of both sides of Eq. (A 3), using then the FP equation for $\partial P/\partial t$ on the left hand-side of the ensuing equation, and finally integrating by parts the terms containing spatial derivatives of P (this procedure results in a closed differential equation for $p_{\text{pot}}(t)$ only if the potential $V(x)$ is harmonic). As every one-dimensional linear first-order differential equation, Eq. (A 4) can be integrated by quadrature, the solution being:

$$p_{\text{pot}}(t) = p_{\text{pot}}(t=0) e^{(k=2k_B) \int_0^t dy D_y = T(y)} + k \int_0^t dt D_{t^0} e^{(k=2k_B) \int_{t^0}^t dy D_y = T(y)}; \quad (\text{A } 5)$$

If we now anneal the temperature down to 0 in a time in the usual way, $T(t) = T_0(1-t^{\tau})^{\tau}$, assuming that the diffusion constant behaves as $D(T) = D_0(T=T_0)^{\alpha}$, we readily get an analytic expression for the residual energy at the end of the annealing, $\text{res}(\tau) = p_{\text{pot}}(t=0)$, which can be shown to behave, for large τ , as a power law :

$$\text{res}(\tau) \stackrel{\text{CA}}{\sim} \frac{T_0}{\tau(D_0-1)+1}; \quad (\text{A } 6)$$

Quite evidently, annealing proceeds here extremely fast, with a power-law exponent CA that can increase without bounds (for instance if $D_0 = 1$) upon increasing the exponent τ of the annealing schedule. Notice, however, that large values of D_0 are, on the contrary, detrimental

2. Quantum Annealing (Schrödinger) case.

Consider now the problem of a particle moving in a parabolic potential $V(x) = kx^2/2$, with a time-dependent mass, such that the Hamiltonian is given by:

$$H(t) = \frac{k}{2}x^2 - (t)r^2; \quad (\text{A } 7)$$

where $\langle t \rangle = \sim^2/2m$ (t) denotes the coefficient of the Laplacian operator. The Schrödinger evolution of the wavefunction $\langle x;t \rangle$ is then,

$$\langle \psi(x;t) = H(t) \langle x;t \rangle; \quad (\text{A } 8)$$

where $= i\sim$ for a real time (RT) evolution, and $= \sim$ for an imaginary time (IT) evolution. Now, whereas general solutions of the time-dependent Schrödinger equation for arbitrary initial condition $\langle x;t=0 \rangle$ are not easy, it turns out that if $V(x)$ is quadratic, then any initial Gaussian wavefunction propagates into a Gaussian, which is enough for our goal. In detail, write the following Ansatz for $\langle x;t \rangle$:

$$\langle x;t \rangle = C_t e^{B_t x^2} \quad \text{Real}(B_t) = \langle B_t \rangle > 0; \quad (\text{A } 9)$$

Substituting the Ansatz for $\langle x;t \rangle$ into the Schrödinger evolution (in RT or in IT), one immediately verifies that $\langle x;t \rangle$ satisfies Eq. (A 8) for arbitrary $\langle t \rangle$ as long as B_t and C_t satisfy the following ordinary differential equations:

$$B_t = k - 2 \langle t \rangle B_t^2; \quad C_t = \frac{C_t}{\langle t \rangle B_t}; \quad (\text{A } 10)$$

Once again, the normalization constant C_t turns out to be irrelevant in calculating the average potential energy

$$p_{\text{pot}}(t) = \frac{\int_{\mathbb{R}} \frac{dxV(x)j(x;t)^2}{dxj(x;t)^2}}{\int_{\mathbb{R}} dxj(x;t)^2} = \frac{k}{4\langle B_t \rangle}; \quad (\text{A } 11)$$

and can be completely forgotten, since the equation for B_t does not involve it. The initial condition $B_{t=0}$ is, by assumption, such that at $t=0$ the system is in the ground state corresponding to $\langle 0 \rangle = \langle t=0 \rangle$. Such a ground state value B_0 is easily calculated by equating to zero the right-hand side of Eq. (A 10) with $\langle t \rangle = 0$, i.e., $B_0 = \sqrt{k/(2B_0)}$.

A few general considerations can be based on a purely qualitative analysis of Eq. (A 10). Consider first the IT case, where the equation for B_t reads $\sim B_t = k - 2 \langle t \rangle B_t^2$. One can easily get convinced that B_t is forced to be a real, positive and monotonically increasing function of t , i.e., $B_t > 0$ and $B_t > 0$ for $t > 0$. Therefore, we can easily write an inequality of the form :

$$\sim B_t = k - 2 \langle t \rangle B_t^2 \geq k;$$

from which we immediately conclude, by integrating over t the two sides of the inequality, that

$$B_t \geq B_0 \frac{k}{\sim};$$

i.e., the residual energy $\text{res}(\tau) = k/(4B_t)$ cannot decrease faster than $1/\tau$ for $\tau > 1$.

We will now assume, without great loss of generality, that the Laplacian coefficient $\langle t \rangle$ is given by $\langle t \rangle = \tau_0(t=0)$, where τ is an annealing time-scale (for instance the annealing time, when a linear schedule is used)

and $f(t^0)$ is a positive decreasing function for $t^0 > 0$ such that $f(t^0 = 0) = 1$. It is useful to switch to dimensionless variables by measuring times in unit of t^0 , $t^0 = t =$, and B_t in units of its initial ground state value $B_{t=0} = B_0$. The appropriate dimensionless quantity is therefore $b(t^0; \beta) = B_t = B_0$, with $t^0 = t =$, where the parametric dependence on the annealing time-scale β has been explicitly indicated. The equation for $b(t^0; \beta)$ is given by:

$$\begin{aligned} b(t^0; \beta) &= [1 - f(t^0)b^2(t^0; \beta)] = \frac{p}{2k_0} = (1) \\ b(0; \beta) &= 1; \end{aligned} \quad (\text{A } 12)$$

where the dot, from now on, will denote a derivative with respect to t^0 . Notice that the parametric dependence on β is all buried into the coefficient b , which reabsorbs also the β appearing in the dynamics (RT versus βT). This kind of non-linear differential equation is of the well-known Riccati form. It can be transformed into a linear second-order differential equation by operating the following substitution

$$b(t^0; \beta) = -\frac{y(t^0; \beta)}{f(t^0)y(t^0; \beta)}; \quad (\text{A } 13)$$

where, evidently, y is defined up to an overall normalization constant. Indeed, simple algebra shows that we can re-express Eq. (A 12) as a second-order linear equation for y , as follows:

$$\begin{aligned} f(t^0)y(t^0; \beta) - f(t^0)y(t^0; \beta) &= -f^2(t^0)y(t^0; \beta) \quad (\text{A } 14) \\ y(0; \beta) &= y(0; \beta); \end{aligned}$$

As long as $f(t^0) \neq 0$, it is simple to verify that the second-order equation for $y(t^0; \beta)$ can be also equivalently written as:

$$\frac{d}{dt^0} \frac{y(t^0; \beta)}{f(t^0)} = -f^2(t^0)y(t^0; \beta); \quad (\text{A } 15)$$

Finally, denoting by $Y(t^0; \beta)$ the indefinite integral of $y(t^0; \beta)$, such that $Y = y$, and integrating over t^0 both sides of Eq. (A 15), we can also write:

$$Y(t^0; \beta) = -\int f(t^0)Y(t^0; \beta) dt^0; \quad (\text{A } 16)$$

Eq. (A 16) is easily solved when the annealing schedule for $f(t)$ is linear, $f(t) = f_0(1 - t)$, i.e., when $f(t) = (1 - t)$ with $f_0 = 1$, a case in which Eq. (A 16) is of the Airy type. In the latter case, it is useful to perform a final change of independent variable to $z = \frac{2}{3}j^{\frac{2}{3}}(1 - t)$, so that, defining $F(z) = Y(t^0; \beta)$, we can write the equation for F in the standard Airy form :

$$\frac{d^2}{dz^2}F(z) = zF(z); \quad (\text{A } 17)$$

The general solution of Eq. (A 17) is given in terms of the two Airy's functions $Ai(z)$ and $Bi(z)$,

$$F(z) = A_i(z) + B_i(z); \quad (\text{A } 18)$$

where A_i and B_i are two constant coefficients. Going back to $Y(t^0; \beta)$ and $y(t^0; \beta)$, we then have the explicit expressions:

$$\begin{aligned} Y(t^0; \beta) &= A_i(\frac{2}{3}j^{\frac{2}{3}}(1 - t)) + B_i(\frac{2}{3}j^{\frac{2}{3}}(1 - t)) \\ Y(t^0; \beta) &= y(t^0; \beta) = \frac{2}{3}j^{\frac{2}{3}}A_i^0(\frac{2}{3}j^{\frac{2}{3}}(1 - t)) + \frac{2}{3}j^{\frac{2}{3}}B_i^0(\frac{2}{3}j^{\frac{2}{3}}(1 - t)) \\ Y(t^0; \beta) &= y(t^0; \beta) = \frac{1}{n}j^{\frac{4}{3}}A_i^0(\frac{2}{3}j^{\frac{2}{3}}(1 - t)) + \frac{1}{n}j^{\frac{4}{3}}B_i^0(\frac{2}{3}j^{\frac{2}{3}}(1 - t)) \\ &= \frac{2}{3}(1 - t)A_i(\frac{2}{3}j^{\frac{2}{3}}(1 - t)) + \frac{2}{3}(1 - t)B_i(\frac{2}{3}j^{\frac{2}{3}}(1 - t)); \end{aligned} \quad (\text{A } 19)$$

where the prime indicates a derivative with respect to z , and we have used the property of Airy's functions that $A_i^0(z) = zA_i(z)$ and $B_i^0(z) = zB_i(z)$. Finally, substituting back the expressions in Eq. (A 19) into the original function B_t , see Eq. A 13, we get:

$$B_t = B_0 \frac{y(t = ; \beta)}{(1 - t =)y(t = ; \beta)} = B_0 j^{\frac{1}{3}} \frac{A_i(\frac{2}{3}j^{\frac{2}{3}}(1 - t =)) + B_i(\frac{2}{3}j^{\frac{2}{3}}(1 - t =))}{A_i^0(\frac{2}{3}j^{\frac{2}{3}}(1 - t =)) + B_i^0(\frac{2}{3}j^{\frac{2}{3}}(1 - t =))}; \quad (\text{A } 20)$$

This general solution correctly depends on one parameter only, i.e., β , so that we can put $\beta = 1$ without loss of

generality. We impose the initial condition $B_{t=0} = B_0$

by requiring:

$$j^{\frac{1}{3}} \frac{A i(\frac{2}{3}j^{\frac{2}{3}}) + B i(\frac{2}{3}j^{\frac{2}{3}})}{A i^0(\frac{2}{3}j^{\frac{2}{3}}) + B i^0(\frac{2}{3}j^{\frac{2}{3}})} = 1 : \quad (A 21)$$

Solving for j , we get:

$$= \frac{\frac{2}{3}j^{\frac{1}{3}} A i(\frac{2}{3}j^{\frac{2}{3}}) - A i^0(\frac{2}{3}j^{\frac{2}{3}})}{\frac{2}{3}j^{\frac{1}{3}} B i(\frac{2}{3}j^{\frac{2}{3}}) - B i^0(\frac{2}{3}j^{\frac{2}{3}})} \quad (A 22)$$

Due to the asymptotic properties of the Airy's functions ($A i(z) \rightarrow 0$, $A i^0(z) \rightarrow 0$ and $B i(z) \rightarrow 1$, $B i^0(z) \rightarrow 1$, when $z \rightarrow 1$ on the real axis), we conclude that for the IT case:

$$! 0 \quad \text{for } (or) \neq 1 \quad (A 23)$$

so that, finally,

$$B(\zeta) = B_0 j^{\frac{1}{3}} \frac{A i(0) + B i(0)}{A i^0(0) + B i^0(0)} \\ \sim B_0 \frac{\frac{2k}{3}}{\frac{1}{3}} \frac{\left(\frac{1}{3}\right)}{\left(\frac{2}{3}\right)} ; \quad (A 24)$$

where we used that $A i(0) = 3^{-2/3} = (2=3)$ and $A i^0(0) = 3^{1/3} = (1=3)$. On the other hand, for the RT case we have to take the limit $z \rightarrow 1$ (on the real axis) instead, and in that region all the Airy's functions oscillate. Nevertheless is possible to show that the value of B is uniformly bounded for $\zeta \neq 1$.

We conclude, therefore, that for large ζ and with a linear annealing schedule, $\zeta = 1$,

$$B(\zeta) \sim \zeta^{\frac{1}{3}} \quad (A 25)$$

and, consequently, the residual energy behaves asymptotically as

$$r_{\text{res}}(\zeta) = \frac{k}{4\zeta(B)} \sim \zeta^{-\frac{1}{3}} : \quad (A 26)$$

The generalization of this result to an arbitrary annealing exponent $\zeta = \zeta(t) = \zeta_0(1-t)$, is a bit more involved. It is however possible to establish a generalization of Eq. (A 26), for arbitrary ζ , that we checked by means of direct numerical integration. It reads:

$$r_{\text{res}}(\zeta) = \frac{k}{4\zeta(B)} \sim \zeta^{\frac{1}{3}} \quad \zeta = \frac{1}{1-t} ; \quad (A 27)$$

an expression that holds true for both RT and IT annealing.

APPENDIX B : CLASSICAL ANNEALING WITH QUANTUM TOOLS: IMAGINARY TIME SCHRÖDINGER EVOLUTION OF THE FOKKER-PLANCK EQUATION.

A side issue, but nonetheless an interesting one we wish to discuss here relates to classical annealing, and con-

cerns the well-known mapping of a Fokker-Planck equation onto an imaginary-time Schrödinger problem²⁴, and its implications on the relationship between CA and QA. The bottom line will be that the mapping does not imply that a FP-based CA is actually equivalent to QA, and moreover that such a mapping is not particularly useful in our annealing context.

Consider, once again, the FP problem with a time-dependent temperature $T(t)$

$$\frac{\partial}{\partial t} P(x; t) = \frac{1}{t} \text{div}(P r V) + D_t r^2 P : \quad (B 1)$$

where both the friction coefficient and the diffusion constant are now time-dependent quantities, which we indicate by $r = r(T(t))$ and $D_t = D(T(t))$. In order to map the problem in Eq. B 1 onto an imaginary-time Schrödinger problem, the standard procedure²⁴ is to pose $P(x; t) = \phi_0(x; t)$ and to determine $\phi_0(x; t)$ in such a way as to eliminate the non-Schrödinger-looking drift term, turning it onto a standard potential term. The algebra is trivial. One can show that the drift term is eliminated if, and only if, the ϕ_0 satisfies the equation:

$$r \phi_0(x; t) = \frac{r V}{2 t D_t} \phi_0(x; t) ;$$

whose solution is readily found to be:

$$\phi_0(x; t) = C(t) e^{V/(2 t D_t)} ; \quad (B 2)$$

with $C(t)$ a function of time only, which can even be taken to be constant without loss of generality. By plugging $P = \phi_0$ in the FP equation B 1, with ϕ_0 as above, one can show that the resulting equation for $\phi_0(x; t)$ is indeed of the Schrödinger form

$$\frac{\partial}{\partial t} \phi_0(x; t) = D_t r^2 \phi_0(x; t) + V_{FP}(x; t) \phi_0(x; t) ; \quad (B 3)$$

with an effective potential V_{FP} given by

$$V_{FP}(x; t) = \frac{1}{2 t} \frac{(r V)^2}{2 t D_t} - r^2 V + \frac{\partial_t \phi_0(x; t)}{\phi_0(x; t)} : \quad (B 4)$$

The first term in V_{FP} is the standard effective potential of the Riccati form obtained in the time-independent case²⁴. The second piece in V_{FP} is absent in the time-independent case, and can be easily seen to be²⁵:

$$\frac{\partial_t \phi_0(x; t)}{\phi_0(x; t)} = V(x) \frac{d}{dt} \frac{1}{2 t D_t} :$$

The main point we want to stress is that, by annealing $T(t)$ and hence D_t , we not only reduce the coefficient of the Laplacian in Eq. B 3, but we also strongly modify the potential V_{FP} , at variance with a genuine QA where only the kinetic term is annealed down. The modifications of the potential are so strong that, at low temperature, the instantaneous eigenvalue spectrum associated to the FP equation, as discussed in Sec. III, is vastly different from that of the quantum double well system.

¹ S. Kirkpatrick, C.D. Gelatt, Jr., M.P. Vecchi, *Science* 220, 671 (1983);

² A.B. Finnila, M.A.Gomez, C.Sebenik, C.Stenson, J.D. Dohol, *Chem. Phys. Lett.* 219, 343 (1994).

³ T.Kadowaki, H.Nishimori, *Phys. Rev. E* 58, 5355 (1998).

⁴ J.Brooke, D.Bitko, T.F.Rosenbaum, G.Aeppli, *Science* 284, 779 (1999).

⁵ E.Farhi, J.Goldstone, S.Gutmann, J.Japan, A.Lundgren, D.Preda, *Science* 292, 472 (2001).

⁶ Y.H.Lee, B.J.Berne, *J. Phys. Chem. A* 104, 86 (2000).

⁷ Y.H.Lee, B.J.Berne, *J. Phys. Chem. A* 105, 459 (2001).

⁸ Giuseppe E.Santoro, Román Martonak, Erio Tosatti, Roberto Car, *Science* 295, p.2427 (2002).

⁹ Román Martonak, Giuseppe E.Santoro, and Erio Tosatti, *Phys. Rev. B* 66, 094203 (2002).

¹⁰ Román Martonak, Giuseppe E.Santoro, and Erio Tosatti, *Phys. Rev. E* 70, 057701 (2004).

¹¹ Demian Battaglia, Giuseppe E.Santoro, and Erio Tosatti, in preparation.

¹² For the Traveling Salesman Problem case, see, for instance, P.F. Stadler and W.Schnabl, *Phys. Lett. A* 161, 337 (1992).

¹³ It is easy to see, by direct substitution in Eq. (3), that, at constant T , the Boltzmann distribution $e^{-V(x)/k_B T}$ is a stationary solution of the Fokker-Planck equation only if D satisfy the Einstein's relation, $(T)D(T) = k_B T$.

¹⁴ N.G. van Kampen, *Stochastic processes in physics and chemistry*, North-Holland, Amsterdam (1987).

¹⁵ If, for instance, $\rho_{\text{res}}(x)$ behaves in one scheme as a power-law, $\rho_{\text{res}}(x) \propto x^{-\alpha}$, and in another as a slowly decreasing logarithm, $\rho_{\text{res}}(x) \propto \log x$, then the first scheme will be sooner or later more convenient independently of most details.

¹⁶ S. Shinomoto and Y.Kabashima, *J. Phys. A* 24 L141 (1991); Y.Kabashima and S.Shinomoto, *J. Phys. Soc. Japan* 60 3993 (1991).

¹⁷ Typically, we restrict the variable x in the interval $[3;3]$, beyond which the potential is too large and $P(x;t)$ is negligible, and use a grid of up to 1000 points, checking for convergence of the results.

¹⁸ D.A.Huse, D.S.Fisher, *Phys. Rev. Lett.* 57, 2203 (1986).

¹⁹ This is generally speaking a difficult task: The estimated value of β is between 0.14 and 0.22, depending on the inclusion of sub-leading corrections, to be compared with the theoretical value of 0.22. Neglecting the log-corrections leads to a wrong estimate of the power-law exponent.

²⁰ L.D.Landau, *Phys. Z. Sowjetunion* 2, 46 (1932).

²¹ C.Zener, *Proc. Royal Soc. A* 137, 696 (1932).

²² For the sake of precision, we should stress the fact that the logarithm is, strictly speaking, born out of the continuum limit, which is indeed valid only for $T > \beta = ka^2/2$. If the lattice constant a is kept finite, there is a minimum non-zero value v for the splitting between the bottom of any two valleys, and, based on the two-level system results, we could anticipate a similar power-law behavior $v^{-\beta}$. Nevertheless, the logarithmic behavior should apply in a whole temperature window with a similar crossover to the power-law behavior.

²³ See, for instance, P.A.Lee and T.V.Ramakrishnan, *Rev. Mod. Phys.* 57, 287 (1985).

²⁴ G.Parisi, *Statistical field theory*, Addison-Wesley (1988).

²⁵ If we consider that $\beta D(t) = k_B T(t)$, we clearly see that, when annealing the temperature, the overall sign of the factor in front of $V(x)$ in the extra term of V_{FP} is negative.